International Journal of Biological Macromolecules 50 (2012) 493–502

Contents lists available at SciVerse ScienceDirect

International Journal of Biological Macromolecules

journal homepage: www.elsevier.com/locate/ijbiomac

A new chitosan–thymine conjugate: Synthesis, characterization and biological activity

Santosh Kumar[a], Joonseok Koh[a,*], Hyerim Kim[a], M.K. Gupta[b], P.K. Dutta[c]

[a] Department of Textile Engineering, Konkuk University, Seoul 143-701, South Korea
[b] Department of Animal Biotechnology, Konkuk University, Seoul 143-701, South Korea
[c] Department of Chemistry, MN National Institute of Technology, Allahabad 211-004, India

ARTICLE INFO

Article history:
Accepted 13 January 2012
Available online 18 January 2012

Keywords:
Chitosan
Thymine-1-yl acetic acid
Acylation
Conjugate
Biomedical applications

ABSTRACT

Conjugation of chitosan with nucleobases is expected to expand its not only antimicrobial activity but also anti-cancer activity. Here, we report the synthesis of a novel chitosan–thymine conjugate by the reaction between chitosan and thymine-1-yl-acetic acid followed by acylation. The synthesized conjugate was characterized by FTIR, XRD, ^{1}H NMR, TGA and SEM. The microbiological screening results demonstrated the antimicrobial activity of the conjugate against bacteria viz., *Escherichia coli*, *Staphylococcus aureus*, and fungi viz., *Aspergillus niger*. The chitosan–thymine conjugate also inhibited ($p < 0.05$) the proliferation of human liver cancer cells (HepG2) in a dose-dependent manner but had no cellular toxicity in non-cancerous mouse embryonal fibroblast cells (NIH 3T3). Thus, the chitosan–nucleobase conjugate may open a new perspective in biomedical applications.

1. Introduction

During the past few decades, there has been an increasing interest in the utilization of nucleobase conjugates with various natural and synthetic biopolymers. Phenanthridinium–nucleobase conjugates [1], metallocene–nucleobase conjugates [2], symmetrical and unsymmetrical α,ω-nucleobase mono- & bis-amide conjugates [3], cyclodextrin–DNA conjugate [4], ferrocene–bis(nucleobase) conjugates [5], neamine–nucleoside conjugates [6], DNA-peptide conjugates [7], peptide–nucleobase conjugates, nucleobase PNA conjugates [8] are few examples that can inhibit the expression a specific DNA or mRNA molecule, inducing a blockade in the transfer of genetic information from DNA to protein either by antigene or antisense strategy. Single stranded domains of DNA and RNA play an essential role in a number of processes in living cells including those involving viruses. Nucleobase-containing peptides, also referred to as nucleopeptides, represent a promising class of molecules of important biomedical significance presenting a peptide-like backbone conjugated to nucleobases through different linker moieties. Recently, Gross et al. have synthesized a bimetallic ruthenocene dicobalt-hexacarbonyl alkyne peptide bioconjugate [9]. Given these benefits, we are interested in modifying the chitosan with nucleobases for their utilization in various biomedical applications. Numerous works have been published on the chemical modification of chitosan [10–18]. This polymer is still being modified to produce various derivatives with improved properties. We have recently demonstrated that chitosan–chloroquinoline conjugate has also potent antimicrobial activity [19]. Several previous studies have synthesized various thymine derivatives and reported potent anti-cancer effect [20–23]. More recently, Manna et al. found that, modification of hyaluronic acid with thymine, by the LBL process, imparted them an anticancer activity [16]. The conjugation of a nucleobase to chitosan may therefore, expand its biomedical utility to include both antimicrobial and anti-cancer action. Chitosan is readily soluble in various acidic solvents, which limits its applications [17]. It has high antimicrobial activity against many pathogenic and spoilage microorganism, including Gram-positive and Gram-negative bacteria and fungi. The exact antimicrobial mechanism of chitosan is still unclear, but several mechanisms have been proposed. The most feasible hypothesis is the leakage of cellular proteins and other intracellular constituents caused by the interaction between the positively charged chitosan and negatively charged microbial cell membranes. Other mechanisms proposed are the inhibition of microbial growth and toxin production by the chelation of essential metals and nutrients, spore components, as well as the penetration of the nuclei of the microorganisms, which leads to the interference of mRNA and protein synthesis. The principle that underlines the anticancer activity of chitosan–nucleobase is conceptually very simple and straightforward. Being an analogue of natural nucleobases, chitosan–nucleobase conjugate may be incorporated into the nuclear DNA during DNA synthesis and into mRNA during transcription. Since chitosan–nucleobase lacks the 3′OH group that is required for the attachment of additional nucleotides, its

* Corresponding authors. Tel.: +82 2 450 3527; fax: +82 2 458 4131.
E-mail address: ccdjko@konkuk.ac.kr (J. Koh).

0141-8130/$ – see front matter © 2012 Elsevier B.V. All rights reserved.
doi:10.1016/j.ijbiomac.2012.01.015

incorporation into DNA or mRNA would induce strand breakage by chain termination leading to cell cycle arrest [24]. Given that cancer cells generally divide faster and have shorter cell cycle, they are likely to be affected by the chitosan–nucleobase more than the non-cancerous or slow dividing cells [25]. The specificity against cancer cells may further be increased by conjugating the chitosan with a polynucleotide whose sequence is complementary to that of oncogene or its mRNA product. In this case, the sequence specific nucleobase of chitosan–nucleobase conjugates will interact with the DNA/mRNA of target site by complementary base pairing (Thymine/Uracil with Adenine and Cytocine with Guanine) and thereby, would inhibit the DNA synthesis and/or mRNA transcription and translation of the cancer causing gene. However, the chitosan–thymine conjugate has not been reported so far as per our knowledge. With this view the present work is directed to the synthesis, characterization and evaluation of the biological activities of the new biopolymer nucleobase conjugate.

2. Experimental

2.1. Materials

The chitosan powder was a product of Qingdao Yunzhou Biochemistry Co. Ltd., China, average molecular weight about <5000 g/mole (Mv) and a degree of deacetylation (DD) of 90%. Thymine (Sigma–Aldrich), KOH (Sigma–Aldrich), bromoacetic acid (Sigma–Aldrich), conc. HCl (Samchun Chemicals, Korea), DCC (Flucka analytical), acetic acid, and ethanol (Dae Jung, Korea) were used without further purification. The antimicrobial test strains, *Escherichia coli* MTCC 739, *Staphylococcus aureus* MTCC 3160, and *Aspergillus niger* MTCC 3537, were arranged from IMTECH, Chandigarh. The purity of all the synthesized compounds has been checked by TLC using silica gel with different solvent systems.

2.2. Synthesis of thymine-1-yl acetic acid

In a 250 mL of round bottomed flask thymine (20 mmol) was dissolved in a solution of potassium hydroxide (80 mmol) in 15 mL of water. While this solution was warmed in a 42 °C in water bath, a solution of bromoacetic acid (35 mmol) in 10 mL of water was added over 30 min. After this, the reaction was stirred for 2 h at this temperature. It was allowed to cool to room temperature (15 °C) and the pH was adjusted to 5.5 with conc. HCl. The solution was then cooled in a refrigerator for 2 h. Precipitate formed was removed by filtration. The solution was then adjusted to pH 2 with conc. HCl and put in a freezer for 5 h. The resulted white precipitate product (Scheme 1) was isolated by filtration, washed with water 2–3 times and dried in vacuum oven at 35 °C for 7 h. The yield 82%, White solid, and m.p. 253–255 °C was obtained according to procedure as described elsewhere [26].

2.3. Synthesis of chitosan–thymine conjugate

To synthesize chitosan–thymine conjugate 100 mg of chitosan powder dissolve in 1% (w/v) hydrochloric acid. The mixture was vigorously stirred by a magnet stirrer at room temperature until the polymer was completely dissolved. 0.294 g thymine-1-yl acetic acid solution was added into the chitosan solution and stirred for 2 h. Then, 0.355 g DCC dissolved in 20 mL of 95% ethanol was added to induce the acylation reaction. The mixture was then stirred for 8 h at room temperature (15 °C). When the reaction finished, the product was then filtered by vacuum and washed with 95% ethanol to remove excessive DCC. The final product (Scheme 1) was dried in vacuum oven at 35 °C for 4 h.

2.4. Measurements

Fourier transform infrared (FT-IR) spectra were recorded on JASCO FT-IR 300E device using KBr. ^{1}H NMR spectra of the samples were recorded on a Bruker 600 MHz NMR spectrometer using tetramethylsilane (TMS) as an internal standard and CD_3COOD and DMSO as a solvent. XRD pattern of the samples were recorded on X-ray diffractometer (D/Max2500VB+/Pc, Rigaku, Japan) with CuKα characteristic radiation (wavelength $\lambda = 0.154$ nm) at a voltage of 40 kV and a current of 50 mA. The scanning rate was 3°/min and the scanning scope of 2θ was from 2° to 45° at room temperature (25 °C). Thermogravimetric analysis (TGA) was carried out in a TA Q 50 system TGA. The samples were scanned from 0 to 800 °C at a heating rate of 10 °C/min under flow of nitrogen. The surface morphology was analyzed by scanning electron microscopy (SEM) JEOLJSM-6490LA. All the spectra were taken in room temperature.

2.5. Antimicrobial activity assay

The antimicrobial activity of the chitosan–thymine conjugate was evaluated by the agar plate disc-diffusion method [27]. Briefly, the solution (0.1%, 0.05% and 0.01%) of the chitosan–thymine conjugate was absorbed in sterilized discs and placed on the lawn cultures of selected microorganisms to assess their antimicrobial activity against one Gram-positive (*S. aureus*), one Gram-negative (*E. coli*) bacteria and one fungus (*A. niger*). The solution (0.1%) of the chitosan only and (0.1%) of thymine only was used for antimicrobial activity. The agar plates were incubated at 37 °C for 24 h and diameters of the inhibitory zone of clearance (mm) surrounding the discs were measured to estimate the antimicrobial activity.

2.6. Assays for cellular cytotoxicity, proliferation, and viability

Mouse embryonic fibroblast cell line (NIH 3T3) and human liver cancer cell line (HepG2) were cultured in Dulbecco's modified Eagle's medium (DMEM, high glucose formulation; Gibco BRL, Grand Island, NY) supplemented with 10% (v/v) fetal bovine serum (Hyclone, Logan, UT), MEM nonessential amino acids (Gibco BRL), 50 μM 2-mercaptoethanol (Sigma–Aldrich Co., St Louis, MO), and chitosan–thymine conjugate (0, 5, 50, 100 μM) for seven days at 37 °C in a humidified atmosphere of 5% CO_2 in air. Non-treated cells and those treated with pure chitosan or thymine (100 μM) were used as controls for comparison. The cells were plated in 24-well plates at an initial seeding density of $2–4 \times 10^4$ cells/mL in triplicates and were evaluated for the rate of cellular toxicity and proliferation by counting the total number of cells every 24 h, as we described earlier [28]. The population doubling time was calculated with the equation $Y_{end} = Y_{start} \times 2(t/T)$, where T is the population doubling time, Y_{start} is the initial cell count, and Y_{end} is the cell count at the end of culture period (t). The rate of cell proliferation (r) was calculated with the equation $r = (\log NH - \log NI)/T2 - T1$, where NH is number of cell harvested, NI is number of cells initially seeded, T1 is the time at seeding (h), and T2 is the time till harvesting (h) [29]. Viability of cells was evaluated based on the esterase enzyme activity and plasma membrane integrity upon FDA (3′6′diacetyl fluorescein diacetate) assay as described earlier [28]. Briefly, cells were washed in Dulbecco's phosphate-buffered saline (DPBS) for 1 min followed by incubation with 2.5 μg/mL FDA stain for 1 min. Stained cells were then washed in PBS to remove the traces of the dye and observed under UV illumination of an epifluorescent microscope fitted with FITC filter set (excitation: 460–490 nm; emission; 515–550 nm; dichromatic: 505 nm). Live cells emitted green fluorescence while dead ones were non-fluorescent. Viability was calculated as the number of green cells/total number of cells × 100. All experiments were repeated three times.

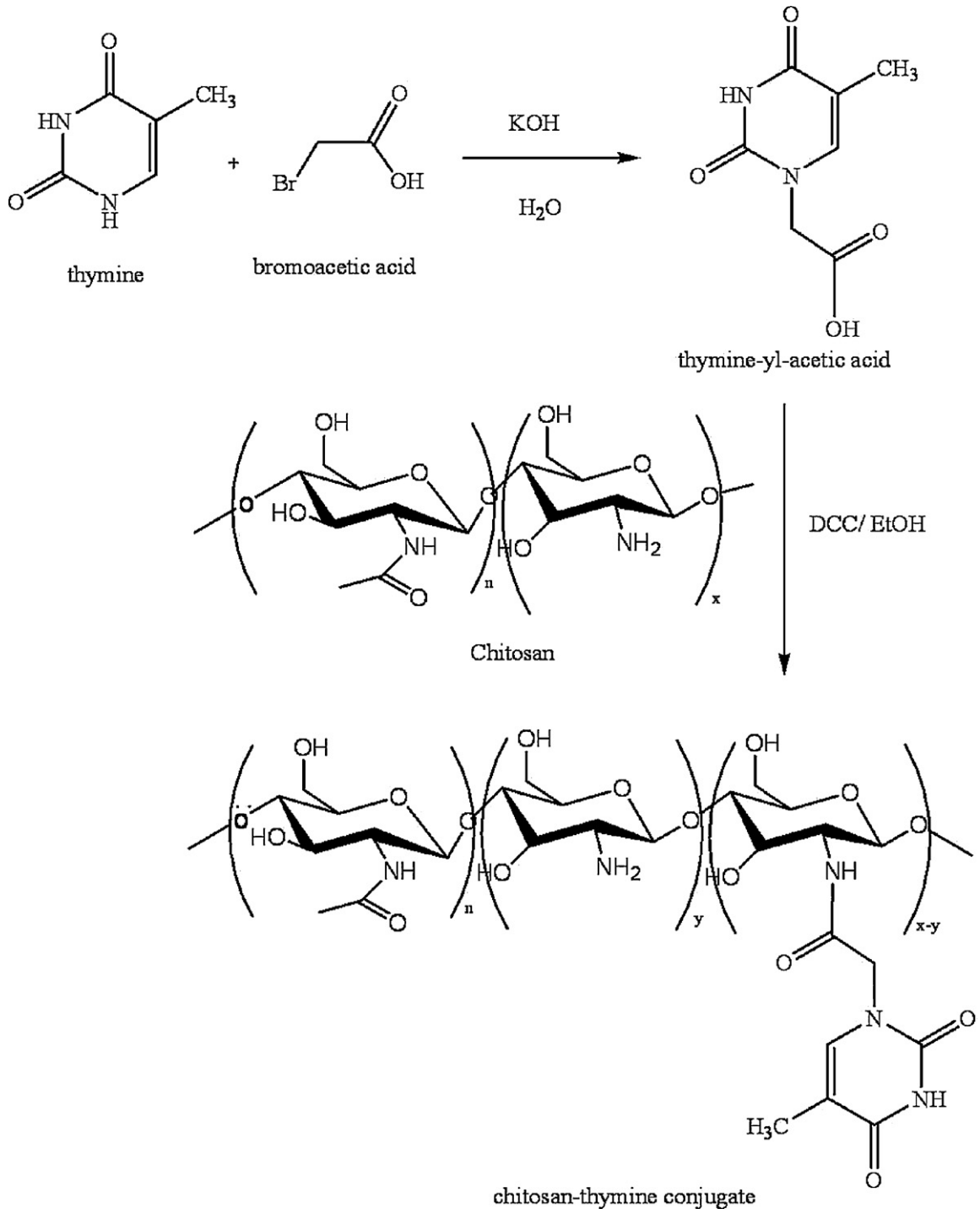

Scheme 1. Synthesis of thymine-1-yl acetic acid and chitosan–thymine conjugate.

3. Results and discussion

Synthesis of thymine modified chitosan is outlined in the Scheme 1. Here, the carboxylic group of modified thymine (thymine-1-yl acetic acid) is reacted with the $-NH_2$ group of chitosan. Manna et al. [16] reported the synthesis of adenine functionalized chitosan by the reaction of —NH of adenine with the primary alcoholic group of chitosan where $-NH_2$ group of chitosan has not been utilized.

3.1. FTIR spectroscopy

FTIR spectra of chitosan, thymine-1-yl-acetic acid and chitosan–thymine conjugate are shown in Fig. 1. Characteristic peaks assignment of chitosan (Fig. 1a) are 3360 cm^{-1} (O—H stretch overlapped with N—H stretch), 2919 and 2874 cm^{-1} (C—H stretch), 1640 cm^{-1} (amide II band, C—O stretch of acetyl group), 1592 cm^{-1} (amide II band, N—H stretch), 1420–1377 cm^{-1} (asymmetric C—H stretch bending of CH_2 group) and 1061 cm^{-1} (skeletal

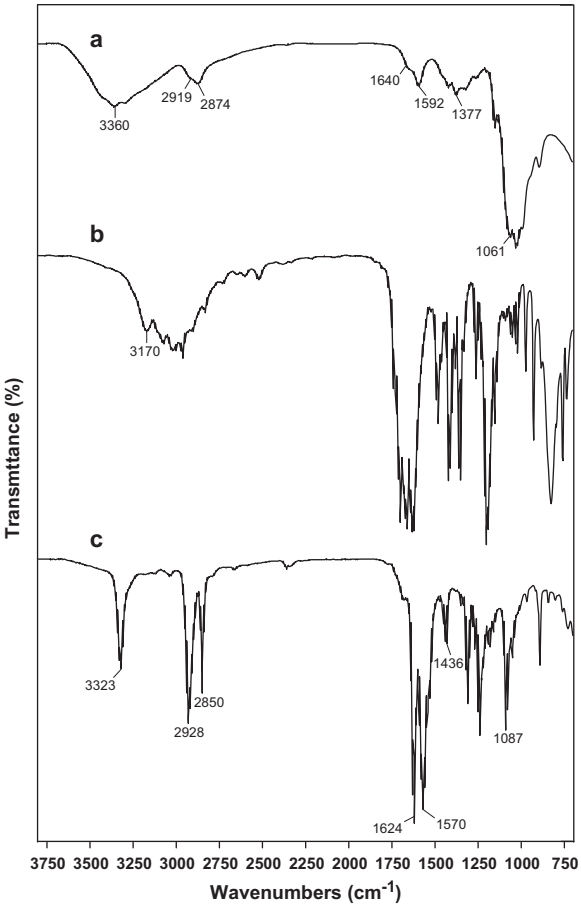

Fig. 1. FTIR spectra of chitosan (a), thymine-1-yl-acetic acid (b), and chitosan–thymine conjugate (c).

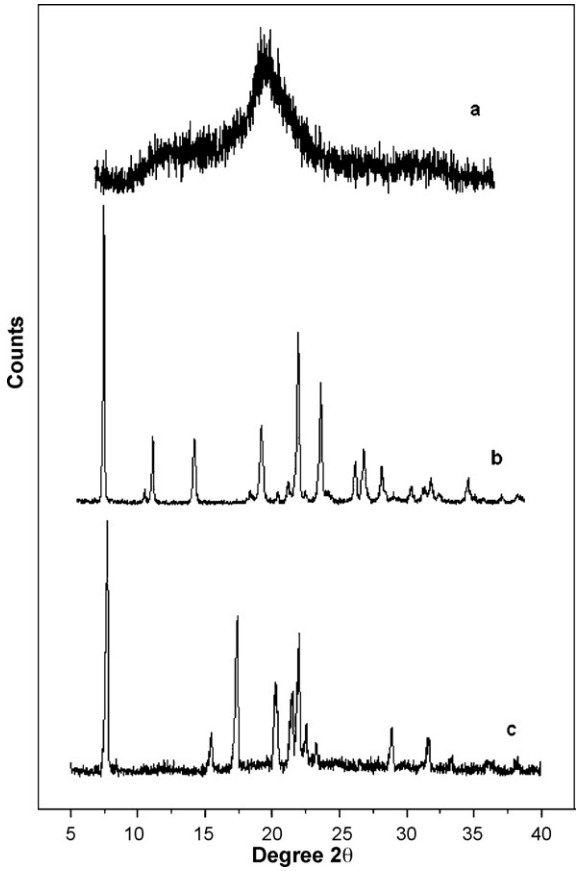

Fig. 2. XRD spectra of chitosan (a), thymine-1-yl-acetic acid (b), and chitosan–thymine conjugate (c).

vibration involving the bridge C—O stretch) of glucosamine residue. The IR spectral band of thymin-1yl acetic acid (Fig. 1b): 3170 cm^{-1} (O—H stretch), 1733–1626 cm^{-1} (C=O stretch). As shown in Fig. 1c the chitosan–thymine conjugate mediated spectral band appear at 3323 cm^{-1} (axial O—H group of chitosan), 2928 and 2850 cm^{-1} (C—H stretch) which were stronger and sharper in comparison to the chitosan. The peaks at 1624 cm^{-1} (amide linkage), 1436 cm^{-1} (C—H stretch bending of CH_2 group), 1570 cm^{-1} (N—H bending stretching) and 1087 cm^{-1} (bridge C—O—C stretch) of chitosan residue were stronger than that of pure chitosan [14a]. The above FTIR analysis clearly indicates that the COOH group of thymin-1-yl acetic acid has been successfully reacted with NH_2 group of chitosan main chain to form amide linkage. The intensity of these bands depends on the amount, type and bulkiness of the acid. Degree of substitution also affects the intensity band, OH which becomes broader on stretching and moves to a higher frequency with increasing DS up to ~60%, indicating an increase in the disordered structure.

3.2. X-ray diffraction spectra

X-ray diffraction spectra of chitosan, thymine-1-yl-acetic acid and chitosan–thymine conjugate are shown in Fig. 2. X-ray diffraction studies of chitosan (Fig. 2a) exhibits very broad peaks at $2\theta = 10^\circ$ and $2\theta = 20^\circ$. Chitosan shows very broad lines especially for the smaller diffraction angles, thereby indicating that long range disorder is found in polymer samples. The broader small angle peaks in chitosan, suggests that conjugate exhibits higher long range order. Diffractive region of thymine-1-yl-acetic acid (Fig. 2b) is observed at 2θ of 7°, 11°, 14°, 19°, 22°, 24°, 26°, 27°, 28° and 31°. The main diffractive region of chitosan–thymine conjugate (Fig. 2c) is at 2θ of 7°, 15°, 17°, 21°, 23°, 28° and 31°. Chitosan–thymine conjugate has higher intensity pattern than chitosan which indicates that the chitosan is substantially more amorphous. Further, the development of high peak intensity for the conjugate is due to the polar group of amide linkage and thus, more number of intermolecular hydrogen bonding. XRD pattern proved here that the crystal lattice has transformed from amorphous structure into a relatively crystalline structure in chitosan–thymine conjugate.

Intensity is not a routine predictor of crystal structure, but can be obtained from XRD pattern and reflects the unit cell dimensions. Intensity is therefore a means of obtaining structural information from powder diffraction. In addition, the lattice dimension is also related to the interplaner distance, *d* can easily be described for the particle size and geometry of the unit cell [34,35].

3.3. ^1H NMR spectra

The ^1H NMR spectra of chitosan, thymin-1-yl acetic acid and chitosan–thymine conjugate were given in Fig. 3. Proton assignment of chitosan in Fig. 3a $\delta = 4.89$ ppm appears for chemical shift of the internal standard, $\delta = 4.37$ ppm is due to chemical shift of the acetal proton (C—H) of glucosamine overlaps the chemical shift of the internal standard, $\delta = 3.27$ ppm for —CH—NH_2 protons (H^2), $\delta = 3.92$–3.72 ppm for (H^3, H^4, H^5 and H^6) protons of glucosamine ring $\delta = 3.27$ ppm appear for chemical shifts of (H^2) proton and upfield $\delta = 2.04$ ppm for (—NHCO—CH_3) acetamido protons. Proton assignment of thymin-1-yl acetic acid shown in Fig. 3b, $\delta = 1.75$ ppm (s, 3H), 4.36 ppm (s, 2H), 7.50 ppm (s, 1H), $\delta = 11.32$ ppm (s, 1H) for N—H, $\delta = 13.10$ ppm (s, 1H) for OH proton of carboxylic acid.

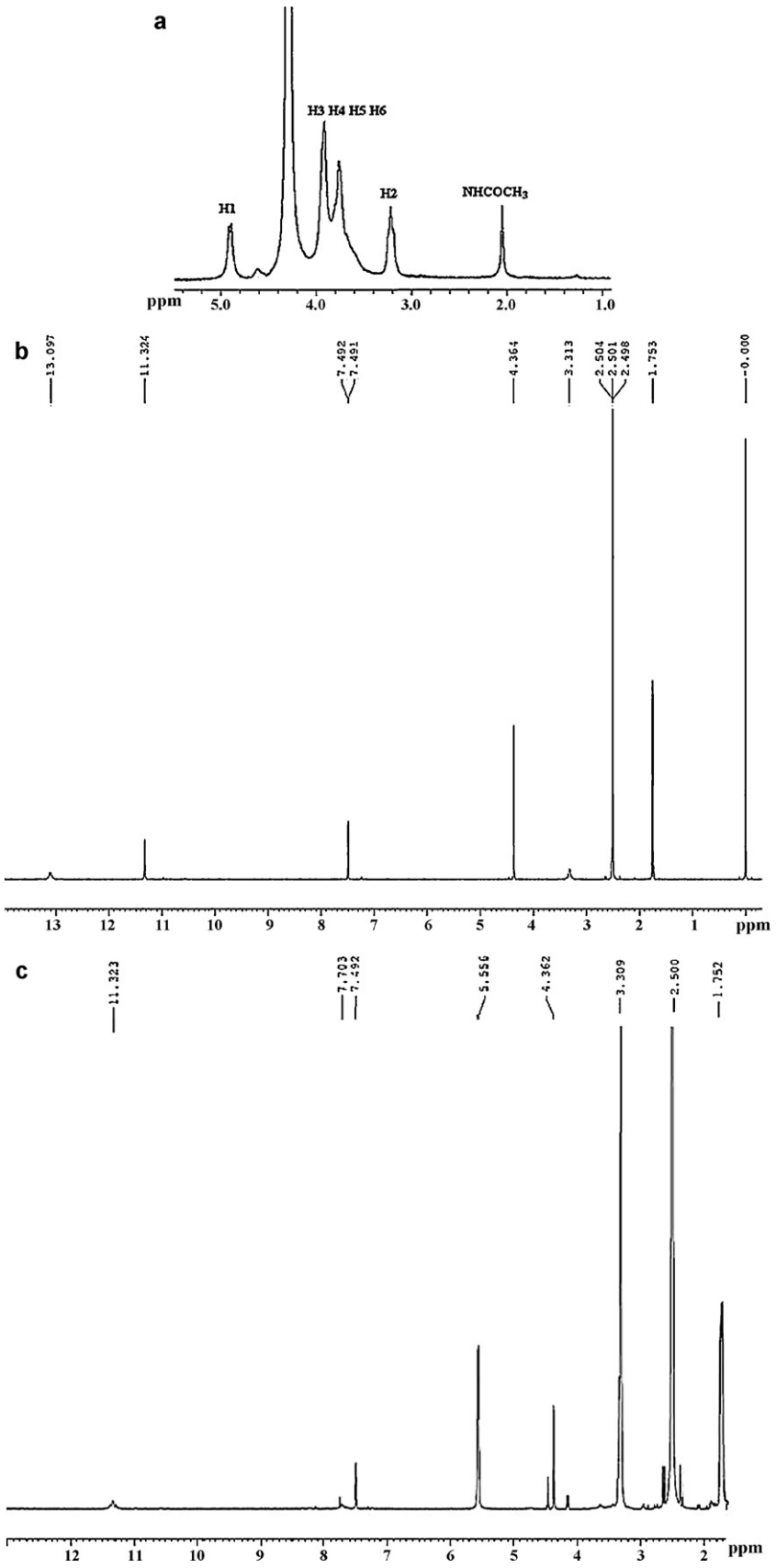

Fig. 3. ^{1}H NMR spectra of chitosan (a), thymine-1-yl-acetic acid (b), and chitosan–thymine conjugate (c).

Compared with chitosan and thymin-1yl-acetic acid, the characteristic proton signals of chitosan–thymine conjugate (Fig. 3c) appeared at $\delta = 5.55$ ppm (s) is due to N—H proton of amide linkage which is formed between NH_2 group of chitosan and COOH group of thymin-1yl acetic acid, $\delta = 7.49$ ppm (s) is CH proton of thymin-1-yl acetic acid, $\delta = 1.75$ ppm (s) CH_3 proton of thymine, $\delta = 11.32$ ppm (s) N—H proton of thymine, and $\delta = 2.50$ ppm (s, $NHCOCH_3$). $\delta = 3.30$ ppm (H-2 of GlcN residue), $\delta = 4.36$ ppm (m) due to glucosamine unit of chitosan. The ^{1}H NMR spectra confirm the formation of new amide linkage between COOH group of thymin-1-yl acetic acid and NH_2 group of chitosan. The degree of modified thymine substitution in chitosan (DS) was found to be 56%. The DS was estimated from the ratio of integral intensity of modified thymine proton to the sum of integral intensities of the chitosan protons.

3.4. Thermogravimetric analysis

The TGA thermograms of chitosan, thymine-1-yl-acetic acid and chitosan–thymine conjugate are shown in Fig. 4. TGA of pure chitosan Fig. 4a showed two different stages of weight loss. The first stage weight loss starting from 47 to 100 °C, this may corresponds to the loss of adsorbed and bound water. The second stage of weight loss starts at 247 °C and continues up to 330 °C due to the degradation of chitosan biopolymer [30]. In Fig. 4c, observed TGA thermogram studies indicate the two weight loss, chitosan–thymine conjugate began to slow weight loss at about 98 °C due to evaporation of water and moisture content in the polysaccharide. At the second stage, A fast process of weight loss appears in chitosan–thymine conjugate decomposing from 180 to 284 °C, is may be due to the lower grafting of acid in a polymer conjugate. It can be seen that thymine-1-yl-acetic acid (Fig. 4b) begins to lose weight around 203 °C. The results demonstrate the loss of the thermal stability for chitosan–thymine conjugate to the chitosan. Introduction of thymine-1-yl-acetic acid group into polysaccharide structure should high degree of crystallinity of conjugate (grafting).

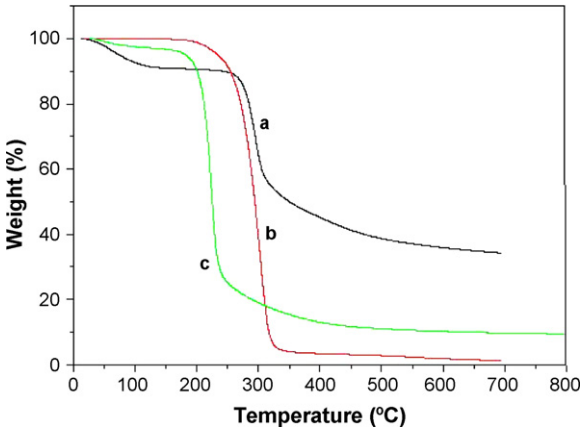

Fig. 4. TGA spectra of chitosan (a), thymine-1-yl-acetic acid (b), and chitosan–thymine conjugate (c).

3.5. Scanning electron microscopy analysis

The scanning electron micrographs (SEMs) of the native chitosan and chitosan–thymine conjugate are shown in Fig. 5. The native chitosan (Fig. 5(a) and (b)) exhibited a nonporous, smooth membranous phase consisting of dome shaped orifices, crystallites and microfibrils. It also exhibited flat lamellar phases on which a large number of protruding microfibrils are evident. The scanning electron micrographs of the chitosan–thymine conjugate are shown in Fig. 5(c) and (d) rough morphology with rod like structure than chitosan. Thymine-1-yl-acetic acid was successfully integrated in to the polymer matrix with no visible agglomerate formation at low particle amounts. The pore dimensions are non-uniform with thin walls and randomly dispersed in the polymer matrix. The rod-like tubes enhance the surface area for better proliferation and better cell adhesion. Further, it enriches for probing DNA-hybridization, antibacterial activity, single nucleotide mutation identification and transfection of living cells. Hence, the surface

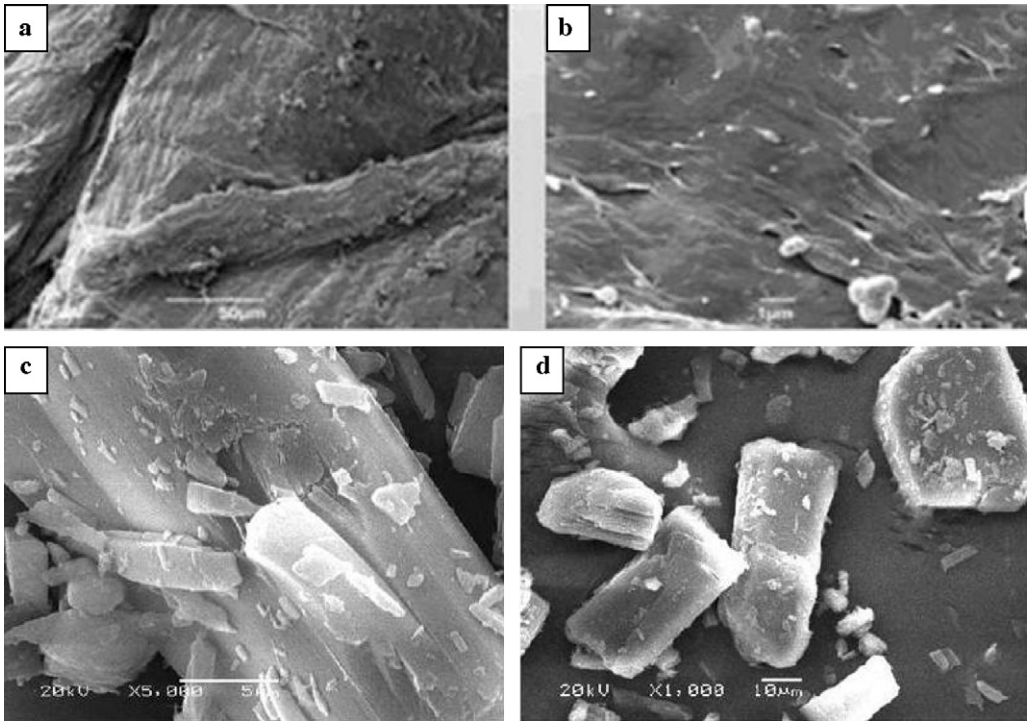

Fig. 5. SEM images of pure chitosan (a), (b) and chitosan–thymine conjugate (c) and (d).

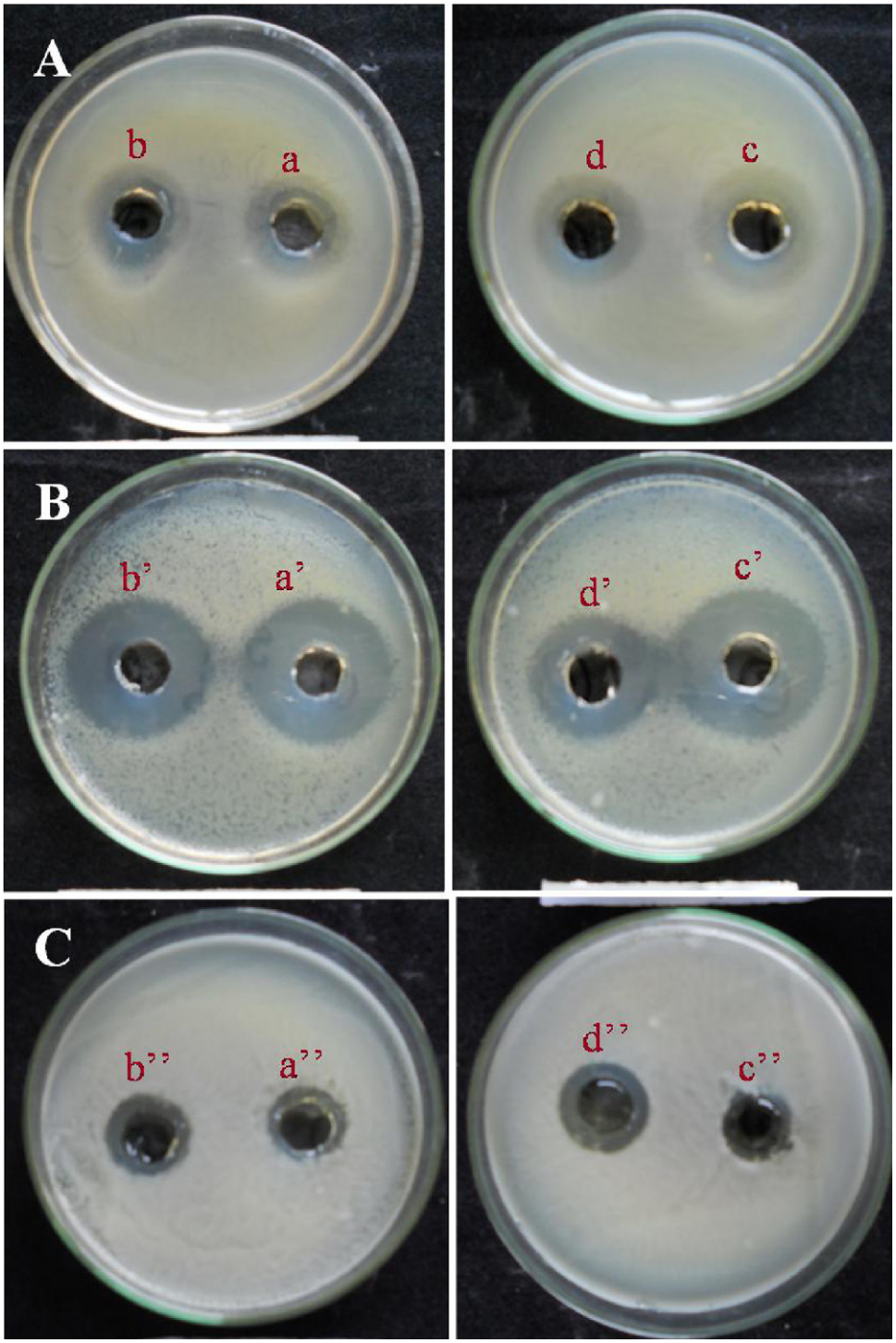

Fig. 6. Inhibitory effect of chitosan–thymine against *E. coli* ((A) a,b,c, and d), *S. aureus* ((B) a′, b′, c′ and d′) and *A. niger* ((C) a″, b″, c″ and d″) in different concentrations 0.1%, 0.05%, 0.01% and control 1% AA respectively.

morphology of the present biopolymeric conjugate has phenomenal impact on its biological property.

3.6. Antimicrobial activity

The inhibitory effect of chitosan–thymine conjugate against *E. coli* ((A) a, b, c, and d), *S. aureus* ((B) a′, b′, c′ and d′) and *A. niger* ((C) a″, b″, c″ and d″) in different concentration 0.1%, 0.05%, 0.01% and control 1% acetic acid respectively are shown in Fig. 6. The diameters of clear inhibition zone around the discs, impregnated with the chitosan–thymine conjugate, were always higher than those of controls for all the tested micro-organisms (Table 1). The diameter of inhibition zone of chitosan only and thymine only were lower than chitosan–thymine conjugate (Table 1). The antibacterial mechanism of chitosan is generally considered due to its positively charged amino group at the C-2 position of the glucosamine

Table 1
The diameters of the inhibitory zone of the chitosan–thymine conjugate, chitosan and thymine in different concentrations.

Bacteria/fungi	Control (1%AA) (mm)	Chitosan–thymine conjugate (mm)			Chitosan (mm)	Thymine (mm)
		0.1%	0.05%	0.01%	0.1%	0.1%
Escherichia coli	22	28	28	27	12	14
Staphylococcus aureus	24	34	32	31	13	15
Aspergillus niger	Not observed	18	17	17	Not observed	13

residue which interacts with negatively charged microbial cell membranes, leading to the leakage of proteinaceous and other intracellular constituents of the microorganisms and thereby, bacterial death [31,32]. There is also a parallel relationship between the antibacterial activity of thymine and its inhibitory action against DNA gyrases in thymine-susceptible clinical isolates of microorganism.

3.7. Assays for cellular cytotoxicity, proliferation, and viability

Finally, we evaluated the effect of the chitosan–thymine conjugate on the cellular viability and proliferation of mouse embryonal fibroblast cells (NIH 3T3) and human liver cancer cells (HepG2) to measure its possible cytotoxicity and anti-cancer activity, respectively. Culture of both NIH 3T3 and HepG2 cells in the presence of the chitosan–thymine conjugate (5, 50, 100 μM), pure chitosan or thymine did not had any adverse affect ($p > 0.05$) on their cellular viability, as measured by cytoplasmic esterase enzyme activity and plasma membrane integrity (Table 2; Fig. 7). These data suggest that the chitosan–thymine conjugate was non-cytotoxic. Interestingly, however, chitosan–thymine conjugate-treated NIH 3T3 and HepG2 cells proliferated slower than non-treated cells and the cells treated with pure chitosan or thymine (Fig. 7). The mean population doubling time was increased while rate of proliferation per day was decreased in a dose-dependent manner in both NIH 3T3 and HepG2 cells cultured in the presence of the chitosan–thymine conjugate (Table 2). This data clearly suggest anti-proliferative action of the chitosan–thymine conjugate. As expected, anti-proliferative action of the chitosan–thymine conjugate was more prominent on cancerous HepG2 cells than on non-cancerous NIH 3T3 cells. The anti-proliferative action was possibly due to DNA strands breaks induced by the incorporation of chitosan–thymine conjugate into the DNA strand during the synthesis phase. Since chitosan–thymine conjugate lacks 3′OH group that is required for the attachment of additional nucleotides during DNA synthesis [24], its incorporation into the newly synthesized DNA molecules might have caused chain termination leading to cell cycle arrest. The increased activity and hence, specificity of chitosan–thymine conjugate on cancerous cells was likely imparted by the rapid rate of cellular proliferation, DNA synthesis and genomic instability in cancer cells [25] which provide increased chance for the incorporation of the chitosan–thymine conjugate in the cancer cells than in the non-cancerous NIH 3T3 cells. Thus, chitosan–thymine conjugate may be suitable as an anti-cancer drug. However, we also observed that HepG2, but not NIH 3T3, cells regained the rate of cellular proliferation upon prolonged culture for 6 days. The cause for this reversibly is currently not clear but has been commonly observed during chemotherapy of most cancers [33]. Taken together, our study suggests the antimicrobial and anticancer action of chitosan–thymine derivatives. Future studies should explore the downstream cell signalling pathways affected by the chitosan–thymine conjugate to result in anti-proliferative action. Our study lay foundation for future study to investigate if the conjugation of an oncogene sequence-specific polynucleotide to the chitosan would impart them enhanced and specific anticancer properties, in addition to antimicrobial action.

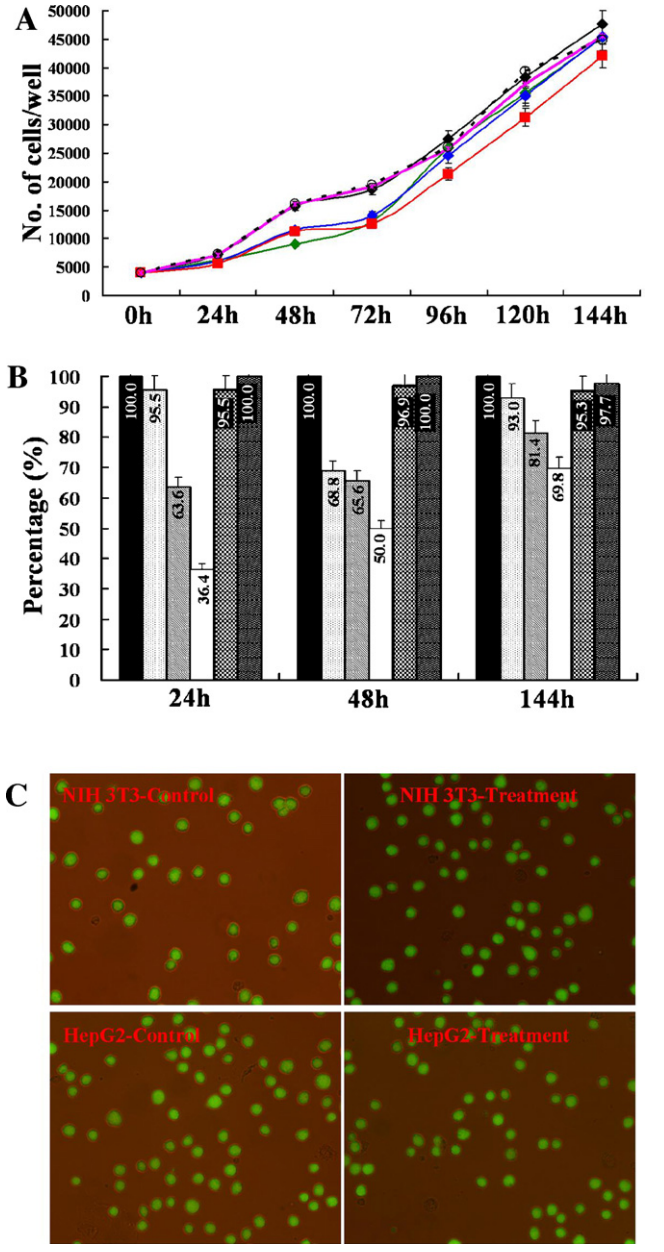

Fig. 7. Cellular proliferation and viability of mouse embryonic fibroblast cell line NIH 3T3 (A) and human liver cancer cell line HepG2 (B) cultured in the absence or presence of chitosan–thymine conjugate and pure chitosan or thymine. A: Proliferation of NIH 3T3 cells cultured in the presence of 0 (black line), 5 (green line), 50 (blue line) or 100 (red line) μM chitosan–thymine conjugate, 100 (pink line) μM chitosan and 100 (dotted line) μM thymine for 144 h. (B) Percentage growth of HepG2 cells cultured in the presence of chitosan–thymine conjugate at different concentration. Values within the bar indicate the percentage of chitosan–thymine conjugate, chitosan and thymine treated cells compared to total number of cells in the non-treated control at 24, 48 and 144 h of culture. (C) Viability of NIH 3T3 and HepG2 cells cultured in the absence or presence of the chitosan–thymine conjugate. Values within the figures indicate the percentage viability measure based on the esterase enzyme activity and plasma membrane integrity by FDA assay. Green fluorescence indicates viable cells. (For interpretation of the references to color in this figure legend, the reader is referred to the web version of the article.)

Table 2
Population doubling time (PDT), cell proliferation rate (r) and viability of mouse embryonic fibroblast (NIH 3T3) and human liver cancer (HepG2) cell line cultured in the presence of chitosan–thymine conjugate, chitosan and thymine at different concentrations.

Groups	Concentration (μM)	PDT (h)		r/day		Viability (%)	
		NIH 3T3	HepG2	NIH 3T3	HepG2	NIH 3T3	HepG2
Control	0	26.67[a]	24.94[a]	0.59[a]	0.65[a]	89.70[a]	96.10[a]
Conjugate	5	30.97[b]	26.12[a]	0.44[b]	0.61[a]	93.20[a]	96.51[a]
Conjugate	50	31.48[b]	39.18[b]	0.42[b]	0.20[b]	94.00[a]	96.71[a]
Conjugate	100	34.29[c]	68.57[c]	0.34[c]	0.16[b]	91.60[a]	95.06[a]
Chitosan	100	27.04[a]	24.92[a]	0.57[a]	0.61[a]	91.60[a]	97.20[a]
Thymine	100	26.30[a]	24.92[a]	0.60[a]	0.65[a]	93.20[a]	98.40[a]

Three replicates were performed. Values with different superscripts (a, b, c) indicate statistical difference ($p < 0.05$).

4. Conclusions

The novel chitosan–thymine conjugate has been successfully synthesized by the acylation reaction between chitosan and thymine-1-yl-acetic acid and its dual antimicrobial and anticancer effect has been tested. The formation of amide bond was confirmed by FTIR, ^{1}H NMR and X-ray diffractometry analysis. The TGA study show that the chitosan–thymine conjugate is thermally stable. The morphological study of the chitosan–thymine conjugate has shown macro porous structure for biomedical properties. The microbiological screening has demonstrated the positive antimicrobial activity against pathogenic bacteria and fungi. The assays for cell proliferation and viability showed that the chitosan–thymine conjugate was non-cytotoxic but significantly reduced the rate of proliferation in cancerous HepG2 cells. Thus, the chitosan–thymine conjugate might be a very promising candidate for practical applications in the field of biomedical and medicine vis-à-vis genetic information (transfer and function).

Acknowledgments

This research was supported by the 2010 KU Brain Pool Program of Konkuk University, Seoul, South Korea. This work was financially supported by the Ministry of Knowledge Economy (MKE) and Korea Institute for Advancement in Technology (KIAT) through the Workforce Development Program in Strategic Technology.

References

[1] L.M. Tumir, M. Grabar, S. Tomic, I. Piantanida, The interactions of bis-phenanthridinium–nucleobase conjugates with nucleotides: adenine-conjugate recognizes UMP in aqueous medium, Tetrahedron 66 (2010) 2501–2513.
[2] A.R. Pike, L.C. Ryder, B.R. Horrocks, W. Clegg, M.R.J. Elsegood, B.A. Connolly, A. Houlton, Metallocene-DNA: synthesis, molecular and electronic structure and DNA incorporation of C5-Ferrocenylthymidine derivatives, Chem. A: Eur. J. 8 (2002) 2891–2899.
[3] S. Boncel, M. Maczka, K.K.K. Koziol, R. Motyka, K.Z. Walczakv, Symmetrical and unsymmetrical alpha,omega-nucleobase amide-conjugated systems, Beilstein J. Org. Chem. 6 (2010), doi:10.3762/bjoc.6.34.
[4] T. Ihara, A. Uemura, A. Futamura, M. Shimizu, N. Baba, S. Nishizawa, N. Teramae, A. Jyo, Cooperative DNA probing using a β-cyclodextrin-DNA conjugate and a nucleobase specific fluorescent ligand, J. Am. Chem. Soc. 131 (2009) 1386–1387.
[5] (a) H.B. Kraatz, Ferrocene-conjugates of amino acids, peptides and nucleic acids, J. Inorg. Organomet. Polym. Mater. 15 (2005) 83–106;
(b) W.A. Wlassoff, G.C. King, Ferrocene conjugates of dUTP for enzymatic redox labeling of DNA, Nucleic Acids Res. 30 (2002) 1–7.
[6] Y. Xu, H. Jin, Z. Yang, L. Zhang, L. Zhang, Synthesis and biological evaluation of novel neamine-nucleoside conjugates potentially targeting to RNAs, Tetrahedron 65 (2009) 5228–5239.
[7] T. Kubo, B. Rumiana, H. Ohba, M. Fujii, Antisense effects of DNA-peptide conjugate, Nucleic Acids Res. Suppl. 3 (2003) 179–180.
[8] G.N. Roviello, E. Benedetti, C. Pedone, E.M. Bucci, Nucleobase-containing peptides: an overview of their characteristic features and applications, Amino Acids 39 (2010) 45–57.
[9] A. Gross, M. Neukamm, N. Metzler-Nolte, Synthesis and cytotoxicity of a bimetallic ruthenocene dicobalt-hexacarbonyl alkyne peptide biconjugate, Dalton Trans 40 (2011) 1382–1386.
[10] (a) S. Kumar, J. Dutta, P.K. Dutta, Preparation and characterisation of N-heterocyclic chitosan derivative based gels for biomedical applications, Int. J. Biol. Macromol. 45 (2009) 330–337;
(b) S. Kumar, N. Nigam, T. Ghosh, P.K. Dutta, S.P. Singh, P.K. Datta, L. An, T.F. Shi, Preparation, characterisation and optical properties of novel azo-based chitosan biopolymer, Mater. Chem. Phys. 120 (2010) 361–370;
(c) S. Kumar, P.K. Dutta, P. Sen, Preparation and characterisation of optical property of crosslinkable film of chitosan with 2-thiophenecarboxaldehyde, Carbohyd. Polym. 80 (2010) 564–570.
[11] S. Kumar, J. Koh, D.K. Tiwari, P.K. Dutta, Optical study of chitosan-ofloxacin complex for biomedical applications, J. Macromol. Sci. A 48 (2011) 789–795.
[12] R.A.A. Muzzarelli, Human enzymatic activities related to the therapeutic administration of chitin derivatives, Cell. Mol. Life Sci. 53 (1997) 131–140.
[13] (a) R. Jayakumar, K.P. Chennazhi, R.A. Muzzarelli, H. Tamura, S.V. Nair, S. Selvamurugan, Chitosan conjugated DNA nanoparticles in gene therapy, Carbohyd. Polym. 79 (2010) 1–8;
(b) R. Jayakumar, N. Nwe, S. Tokura, H. Tamura, Sulfated chitin and chitosan as novel biomaterials, Int. J. Biol. Macromol. 40 (2007) 175–181;
(c) R. Jaykumar, M. Prabaharan, S.V. Nair, H. Tamura, Novel chitin and chitosan nanofibers in biomedical applications, Biotechnol. Adv. 28 (2010) 142–150.
[14] (a) M.K.S. Batista, L.F. Pinto, C.A.R. Gomes, P. Gomes, Novel highly soluble peptide–chitosan polymers: chemical synthesis and spectral characterization, Carbohydr. Polym. 64 (2006) 299–305;
(b) N.M. Alves, J.F. Mano, Chitosan derivatives obtained by chemical modifications for biomedical and environmental applications, Int. J. Biol. Macromol. 43 (2008) 401–414.
[15] V.K. Mourya, N.N. Inamdar, Chitosan-modification and applications: opportunities galore, React. Funct. Polym. 68 (2008) 1013–1051.
[16] U. Manna, S. Bharani, S. Patil, Layer-by-layer self-assembly of modified hyaluronic acid/chitosan based on hydrogen bonding, Biomacromolecules 10 (2009) 2632–2639.
[17] (a) R. Jayakumar, M. Prabaharan, R.L. Reis, J.F. Mano, Graft copolymerized chitosan present status and applications, Carbohyd. Polym. 62 (2005) 142–158;
(b) R. Jayakumar, H. Nagahama, T. Furuike, H. Tamura, Synthesis of phosphorylated chitosan by novel method and its characterization, Int. J. Biol. Macromol. 42 (2008) 335–339;
(c) R. Jayakumar, H. Tamura, Synthesis, characterization and thermal properties of chitin-g-poly(ε-caprolactone) copolymers by using chitin hydrogel, Int. J. Biol. Macromol. 43 (2008) 32–36.
[18] (a) R. Jayakumar, M. Prabaharan, P.T.S. Kumar, S.V. Nair, H. Tamura, Biomaterials based on chitin and chitosan in wound dressing applications, Biotechnol. Adv. 29 (2011) 322–337;
(b) N.S. Rejinold, K.P. Chennazhi, S.V. Nair, H. Tamura, R. Jayakumar, Biodegradable and thermo-sensitive chitosan-g-poly(N-vinyl-caprolactam) nanoparticles as a 5-fluorouracil carrier, Carbohyd. Polym. 83 (2011) 776–786.
[19] S. Kumar, P.K. Dutta, J. Koh, A physico-chemical and biological study of novel chitosan–chloroquinoline derivative for biomedical applications, Int. J. Biol. Macromol. 49 (2011) 356–361.
[20] N. Borg, X.X. Zhou, N.G. Johansson, B. Oberg, L. Stahle, Distribution to the brain and protein binding of 3′ and 5-substituted 2′,3′-dideoxyuridine derivatives studied by microdialysis, Antiviral Chem. Chemother. 8 (1997) 47–53.
[21] X.-J. Liu, R.-Y. Chen, Synthesis of novel phosphonotripeptides containing uracil or thymine group, Phosphorus, Sulfur Silicon 176 (2001) 19–28.
[22] H. Tanaka, H. Takashima, M. Ubasawa, K. Sekiya, N. Inouye, S. Shigeta, R.T. Walker, De Clercq, E.T. Miyasaka, Synthesis and antiviral activity of 6-benzyl analogs of 1-[2-Hydroxyethoxy] methyl]-5-(phenylthio) thymine (HEPT) as potent and selective anti-HIV-1 agents, J. Med. Chem. 38 (1995) 2860–2865.
[23] G.N. Roviello, S.D. Gaetano, D. Capasso, S. Franco, C. Crescenzo, E.M. Bucci, C. Pedone, RNA-binding and viral reverse transciptase inhibitory activity of a novel cationic diamino acid based peptide, J. Med. Chem. (2011), doi:10.1021/jm1012769.
[24] D.L. Nelson, M.M. Cox, DNA replication, in: Lehninger Principles of Biochemistry, 4th ed., 2005, pp. 950–966.
[25] D. Hanahan, R.A. Weinberg, Hallmarks of cancer: the next generation, Cell 144 (2011) 646–674.

[26] A.R. Katritzky, T. Narindoshvili, Chiral peptide nucleic acid monomers (PNAM) with modified backbones, Org. Biomol. Chem. 6 (2008) 3171–3176.
[27] C.L. Clark, M.R.J. Jacobs, P.C. Appelbaum, Antipneumococcal activities of levofloxacin and clarithromycin as determined by agar dilution, microdilution, E-test, and disk diffusion methodologies, J. Clin. Microbiol. 36 (1998) 3579–3584.
[28] Z.C. Das, M.K. Gupta, S.J. Uhm, H.T. Lee, Increasing histone acetylation of cloned embryos, but not donor cells, by sodium butyrate improves their in vitro development in pigs, Cell Reprogram. 12 (2010) 95–104.
[29] Y.H. Jung, M.K. Gupta, S.H. Oh, S.J. Uhm, H.T. Lee, Glial cell line derived neurotrophic factor alters the growth characteristics and genomic imprinting of mouse multipotent adult germline stem cells, Exp. Cell Res. 316 (2010) 747–761.
[30] C. Peniche, W. San Roman Arguelles-Monal, A kinetic study of the thermal degradation of chitosan and a mercaptan derivative of chitosan, Polym. Degrad. Stab. 39 (1993) 21–28.
[31] M.F.A. Goosen, Applications of Chitin and Chitosan, Technomic Publishing Inc, Lancaster, 2001, p. 131.
[32] L.Y. Zheng, J.F. Zhu, Study on antimicrobial activity of chitosan with different molecular weights, Carbohyd. Polym. 54 (2003) 527.
[33] B.C. Baguley, Multiple drug resistance mechanisms in cancer, Mol. Biotechnol. 46 (2010) 308–316.
[34] W. Clegg (Ed.), The intensity of diffracted X-rays, Oxford Science Publication, 1998, p. 21.
[35] T. Ungár, Characterization of nanocrystalline materials by X-ray line profile analysis, J. Mater. Sci. 42 (2007) 1584–1593.